Superconductivity in high-pressure solids

2007 J. Phys.: Condens. Matter 19 425208

(http://iopscience.iop.org/0953-8984/19/42/425208)

IOP PUBLISHING JOURNAL OF PHYSICS: CONDENSED MATTER

J. Phys.: Condens. Matter **19** (2007) 425208 (8pp) doi:10.1088/0953-8984/19/42/425208

Superconductivity in high-pressure solids

John S Tse[1], Yansun Yao[1] and Yanming Ma[2]

[1] Department of Physics and Engineering Physics, University of Saskatchewan, Saskatoon, SK, S7N 5E2, Canada
[2] National Laboratory for Superhard Materials, Jilin University, Changchun 130012, People's Republic of China

Received 3 August 2007
Published 18 September 2007
Online at stacks.iop.org/JPhysCM/19/425208

Abstract

The structural principle behind the unusual features in the high-pressure phases of simple alkali elements is reviewed. It is shown that there exists a pressure regime in which the elemental solids are likely to adopt a layer structure. There are two novel characteristics associated with this structure type. The system tends to be at the proximity of phonon and electronic instabilities. The combined effect is a significant enhancement of electron–phonon coupling, resulting in a superconducting state. We demonstrate this empirical observation with selected examples including a recently predicted novel structure of high-pressure SnH_4 which shows very high superconducting critical temperature.

(Some figures in this article are in colour only in the electronic version)

1. Introduction

One of the most interesting properties of high-pressure solids is the ubiquitous presence of superconducting states in the high-pressure phase(s) [1]. The theoretical prediction and experimental confirmation of elemental Si [2, 3] (a semiconductor under ambient condition) with a fairly high superconducting critical temperature T_c of 9 K at 15 GPa (Si-V) over 20 years ago was a remarkable feat. Over the years, more solids were found to be superconducting in the high-pressure phase. This list includes insulating and metallic elements [1] and even ionic solids [4]. Moreover, there seems to be no restriction on the structural types. Superconducting states have been observed in well-formed crystals and also in modulated incommensurate structures [5]. Most surprising recent findings are the observation of superconductivity in Li in the face-centred cubic (fcc) phase [6–8] and in the non-magnetic state of hexagonal close-packed (hcp) ε-Fe [9]. In the case of Li, T_c up to 17 K has been reported at a relatively low pressure of 37 GPa. Recently, the values of T_c for Ca at 160 GPa and Y at 115 GPa were found to be surprisingly high, at 25 K [10] and 19.5 K [11], respectively. The observation of superconductivity in simple metals such as Li, Ca, and Y poses a challenge to the conventional wisdom, such as Matthias's rule [12], which states that the occurrence of superconductivity is most favourable in systems rich in valence electrons.

Theoretical calculations on high-pressure solids have shown that the superconducting behaviour in high-pressure solids can generally be explained by phonon-mediated strong coupling Migdal–Eliashberg theory [13, 14] within the framework of the Bardeen–Cooper–Schrieffer (BCS) model [15]. The Allen–Dynes modification of the McMillan equation [16] is often used to estimate the superconducting critical temperature T_c,

$$T_c = \frac{\omega_{\log}}{1.2} \exp\left[-\frac{1.04\,(1+\lambda)}{\lambda - \mu^*(1+0.62\lambda)}\right] \tag{1}$$

where λ is the electron–phonon coupling (EPC) parameter or enhancement factor, $\omega_{\log}$ is the phonon frequencies' logarithmic average and μ^* the Coulomb pseudopotential. Moreover, λ is related to twice of the first inverse moment of the Eliashberg spectral function $\alpha^2F(\omega)$ [14],

$$\lambda = 2\int_0^\infty \frac{\alpha^2F(\omega)}{\omega}\,\mathrm{d}\omega. \tag{2}$$

The Eliashberg spectral function $\alpha^2F(\omega)$ is the central quantity of the Migdal–Eliashberg theory. It is defined in terms of the phonon linewidth γ_{qj} of mode j at wavevector q by

$$\alpha^2F(\omega) = \frac{1}{2\pi N(\varepsilon_F)} \sum_{qj} \frac{\gamma_{qj}}{\omega_{qj}} \delta(\omega - \omega_{qj}), \tag{3}$$

where ω_{qj} is the phonon frequency and $N(\varepsilon_F)$ the electronic density of states per atom and per spin at the Fermi level ε_F. γ_{qj} arising from electron–phonon interaction is given by [17]

$$\gamma_{qj} = \frac{4\pi\omega_{qj}}{N_k} \sum_{knm} \left|g^j_{kn,k+qm}\right|^2 \delta(\varepsilon_{kn})\delta(\varepsilon_{k+qm}), \tag{4}$$

where the sum is over the first Brillouin zone (BZ), N_k is the number of k points in the sum, and the ε_{kn} are the energies of bands measured with respect to the Fermi level at point k. $g^j_{kn,k+qm}$ is the electron–phonon matrix element. The contribution of each vibrational mode to the EPC parameter is defined as $\lambda_{qj} = \gamma_{qj}/\pi\hbar N(\varepsilon_F)\omega^2_{qj}$. The EPC parameter λ is the summation of λ_{qj} over all phonon modes (qj) in the first BZ.

$$\lambda = \sum_{qj} \lambda_{qj} w(q) \tag{5}$$

where $w(q)$ is the weight of a sampling q point in the first BZ.

From the inspection of equation (1) and assuming μ^* is a constant (in the strong coupling limit $\mu^* \approx 0.1$), then T_c is directly proportional to the average vibrational spectrum, but it also depends exponentially on λ. Therefore, it is not always necessary that superconductivity will be favourable in systems with high vibrational frequencies and high electron density of states (DOS) at the Fermi level. In some special cases, the presence of low-frequency vibrations, for example acoustic modes that couple strongly with the electrons, may also help to enhance the T_c. In the seminal theoretical investigation on Si-V [2, 3], it was recognized that the presence of a soft transverse acoustic mode together with covalent Si bonds resulted in a local field which enhances the electron–phonon attraction.

In this paper, the relationship between the structure and the electronic structure and phonon spectrum at high pressure will be discussed, using results drawn from recent theoretical studies selected from the work of the authors. It is shown that, upon compression, both metals and insulators often go through an intermediate phase in which the valence orbitals rehybridize and the electrons partially localize, resulting in structures with reduced bonding dimensionality, such as two-dimensional (2D) layered or 1D chain-like structures. Features of these structures are the presence of low-frequency interplanar vibrations and an electronic band structure favourable for electron transport.

2. Results and discussions

2.1. Structural change under pressure

The conventional wisdom is that when an elemental solid, for example, a simple metal, is compressed, it will adopt increasingly close-packed structures. Recent experiments on alkali metals, notably Rb [18, 19] and Cs [20], demonstrated that in the intermediate-pressure regime, very complex structures and sometimes open structures can be formed. The simple picture of compressing hard spheres is, of course, only valid if no change in the electronic structure is taken into account. In reality, compression will lead to extensive mixing of the filled and empty states in both metals and insulators. This is nicely demonstrated in the analysis of the topology of valence electron density in Si [21][3]—a covalent solid under pressure. It was shown [21] (see footnote 3) that, during successive structural phase transformations, the participation of predominantly d conduction bands becomes progressively more important. In a chemical or localized description, the spatially diffused d orbitals provide the flexibility for the electrons to delocalize, and the system becomes more metallic. However, 'covalent' bonding between the Si atoms can still be clearly identified until beyond the stability range of Si-VI [22]. The directional covalent bonds facilitate the stability of the open-structure of Si-VI [22]. At higher pressure, when the system becomes fully metallic, the 'normal' close-packed hcp [23] and fcc [24] structures become favourable again. In essence, the results showed that, upon compression, the dimensionality of the high-pressure phases of Si reduces gradually from 3D to 2D to 1D and eventually to 0D [21] (see footnote 3). A similar transformation sequence is also observed in metallic Rb and Cs. At low pressure, the system behaves like an almost free-electron system and the 'metallic' binding is isotropic and non-directional. However, at the onset of the Cs-II (fcc) to Cs-III transformation, the partial mixing of the 5d states resulted in complex modulated or even intercalated structures. A unique feature of these complex structures is that the chemical 'bonding' or interactions are no longer three-dimensional. In fact, these structures can be described as the stacking of 2D layers. Interestingly, the structural motif of these complex structures with increasing pressures parallels that of 2D Archimedean tiling [25] with increasing packing density. Archimedean tiling (or uniform tiling) is plane tiling of edge-to-edge packing of regular polygons. There are 11 different types of Archimedean tiling, and each can be denoted by the symbol $(p_1^{q_1}, p_2^{q2} \ldots p_n^{q_n})$, with $p_1, p_2 \ldots p_n$ denoting regular p-gons, and $q_1, q_2 \ldots q_n$ the number of adjacent regular p-gons of the same type which are incident with one vertex. A schematic diagram showing the structural changes is illustrated in figure 1. For example, starting from the fcc square-net structure (4^4) of Rb-II and Cs-II, the 3^34^2 layer is observed in Rb-III [18] and Cs-III [20]. Upon compression, the 4.8^2 network is observed in the framework of Rb-IV [19] with the intercalated Rb atoms situated along the channel running down the centre of the large octagon, and the distribution is incommensurate with the framework [19]. It is easy to identify that the $3^2$4.3.4 network is adopted by the Cs atoms in the Wyckoff 8f positions in the Cs-V structure [26]. Eventually, at the highest pressure, Cs adopts the close-packed hexagonal network 3^6 (the hcp structure of Cs [27]).

The simplistic energy level diagram shown in figure 2 helps to rationalize the changes in atom valence electron distribution (rehybridization) under pressure. At high pressure, the empty d states become available for additional (and directional) bonds. Since there are now more orbitals for bonding than available valence electrons, the electrons can preferentially occupy some of the orbitals. In the case of Rb-III and Cs-III, s–d mixing resulted in the localization of the electrons in the centre of the 'squares' in the 3^34^2 network forming the layer structures [21]

[3] A discussion of the structural transformation sequence in alkali metals at high pressure based on a displacive mechanism has been presented in Katzke and Toledano [21].

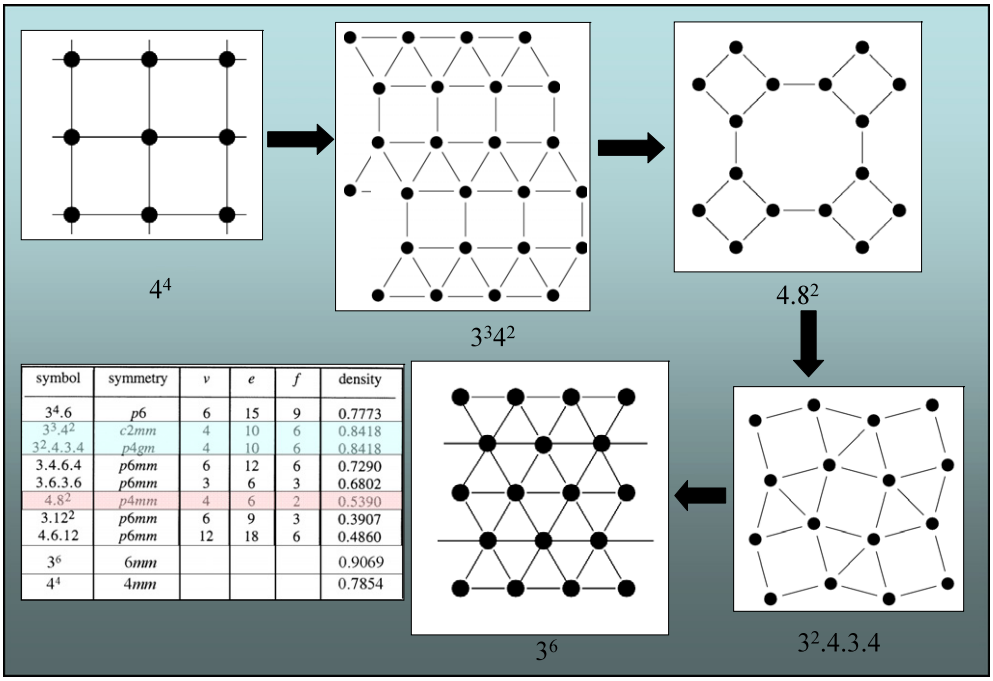

symbol	symmetry	*v*	*e*	*f*	density
$3^4.6$	*p6*	6	15	9	0.7773
$3^3.4^2$	*c2mm*	4	10	6	0.8418
$3^2.4.3.4$	*p4gm*	4	10	6	0.8418
3.4.6.4	*p6mm*	6	12	6	0.7290
3.6.3.6	*p6mm*	3	6	3	0.6802
4.8^2	*p4mm*	4	6	2	0.5390
3.12^2	*p6mm*	6	9	3	0.3907
4.6.12	*p6mm*	12	18	6	0.4860
3^6	*6mm*				0.9069
4^4	*4mm*				0.7854

Figure 1. 2D Archimedean tiling pattern for planar close-packed structures. The table shows the calculated 2D packing densities.

(see footnote 3). An important feature of the 2D directional bonding is that the electronic bands also depend on the crystal directions. It is expected that along the 2D planes the electron bands will be less dispersive due to weak covalent interactions. In comparison, the electron bands perpendicular to the planes will be more free-electron like and probably responsible for the metallic conductivity. As will be shown later, this characteristic band structure may have an important consequence to potential superconductivity behaviour.

2.2. Phonon and electron–phonon coupling

A consequence of the formation of a layered structure is the possible occurrence of low-frequency vibrational modes. This has been shown previously in Si-V [2, 28]. Another example is Si-VI [28]. It was shown that the interplanar vibrational mode can become soft and anharmonic and the structure is, in fact, only entropically stable [28]. Another interesting observation made in Si-VI is the possible occurrence of an electronic instability due to nesting of the Fermi surface [28]. The unprecedented superconductivity in the fcc phase of Li has been attributed to the simultaneous existence of dynamical (phonon) and electronic instability [29–31]. In Li, the soft acoustic mode arises from the shear motion of the lattice [29]. The mode softening is a manifestation of the weakening of interlayer interactions. At 38 GPa, fcc Li transforms into a more complex cubic form (cI16) in which the 2D 3^34^2 pattern is clearly identifiable in the [110] plane. On the other hand, close to the phase transition, the spherical free-electron-like Fermi surface distorts and forms interconnected 'necks' [29, 31, 32]. Moreover, parallel electronic bands start to develop in the [110] plane, indicating a possible nesting of the Fermi surface in the $\Gamma \rightarrow$ K direction (figure 3). The large electron–phonon coupling is associated with this electronic instability. Theoretical

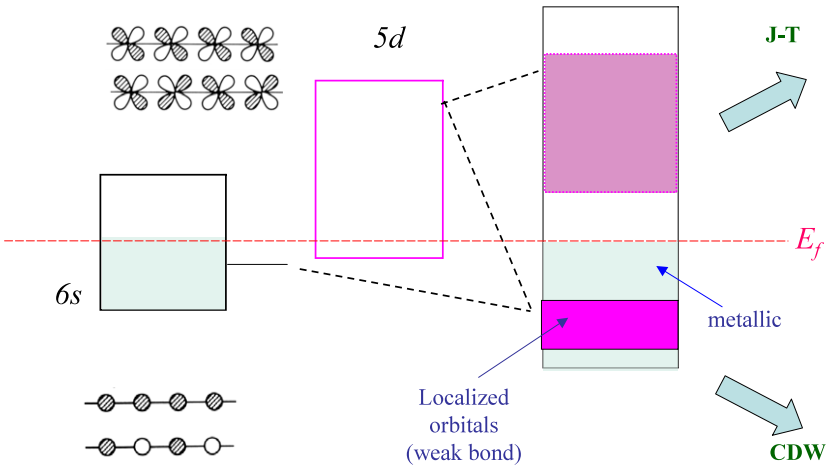

Figure 2. A schematic energy level diagram illustrating changes in chemical bonding pattern as a result of the participation of d states from the conduction band for an alkali metal.

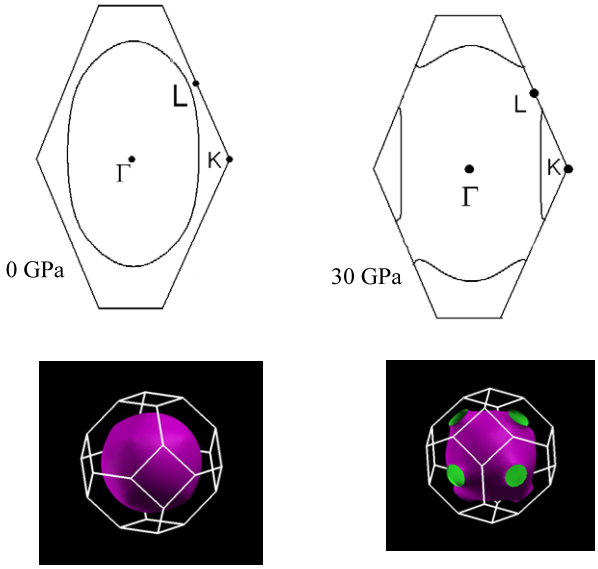

Figure 3. Distortion of the Fermi surface of fcc Li under pressure. Note the nesting of Fermi surface in the $\Gamma \rightarrow$ K direction at 30 GPa.

calculations [29] on fcc Li confirm that the largest contribution to the electron–phonon coupling is due to a soft transverse acoustic mode in the $\Gamma \rightarrow$ X and X $\rightarrow$ L directions.

2.3. A designer high-pressure superconductor

Having discussed the favourable parameters contributing to the superconducting state, a challenge is whether one can design a superconductor at high pressure. Recently, from simulated annealing *ab initio* molecular dynamics simulations, a novel high-pressure phase of SnH_4 has been obtained. Details of the calculations have been presented elsewhere [33]. This

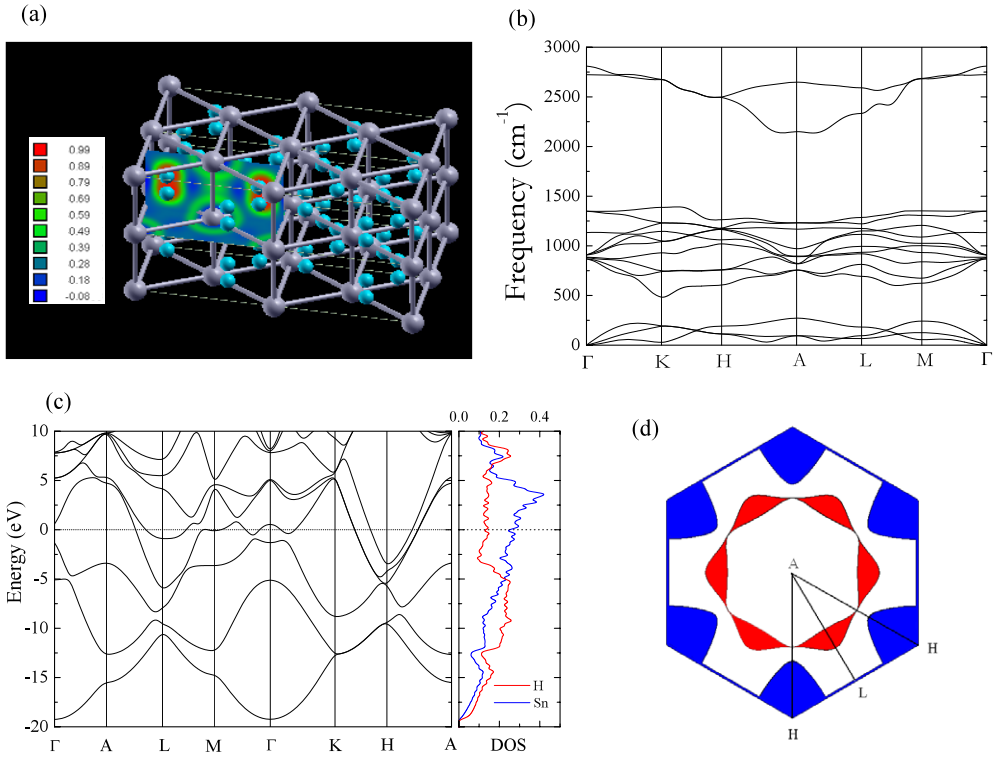

Figure 4. (a) Structure of the hexagonal phase of SnH_4 at 120 GPa. The (colour) contours show the values of the electron localization function. Note the strong electron localization between the H atoms. (b) The phonon band structure. (c) The electronic band structure and (d) the Fermi surface showing possible nesting directions.

structure, dynamically stable between 70–160 GPa, has a hexagonal arrangement of layers of Sn atoms with pairs of hydrogen atoms situated between the layers. At 120 GPa, the H $\cdots$ H separation is found to be only 0.849 Å, which may be too long to be regarded as a normal H–H bond. An analysis of the topology of the electron density (figure 4(a)) indicated that there are strong H $\cdots$ H and weaker Sn $\cdots$ H interactions. These interactions led to high-frequency localized H $\cdots$ H stretch and low-frequency Sn $\cdots$ H translational vibrations (figure 4(b)). Four soft acoustic modes were identified at the K and M symmetry points and along the H $\rightarrow$ A and A $\rightarrow$ L directions (figure 4(b)). The electronic band structure (figure 4(c)) shows, near the Fermi level, highly dispersive bands along K $\rightarrow$ H $\rightarrow$ A and less dispersive bands from M $\rightarrow$ Γ $\rightarrow$ K. Moreover, two sets of almost parallel bands were found along K $\rightarrow$ H and H $\rightarrow$ A, respectively (figure 4(d)). The features in the electronic and phonon band structure suggest that this novel SnH_4 structure may be superconducting [34]. Detailed electron–phonon calculations confirm this speculation. From the calculated phonon linewidths, it is shown that indeed the phonons at K, L $\rightarrow$ A and H $\rightarrow$ A contribute mostly to the electron–phonon coupling mechanism. Detailed investigation on the Fermi surface using the nesting function (bare susceptibility) [31, 35]

$$\xi(q) = \frac{1}{N_k} \sum_{nm} \sum_{k} \delta(\varepsilon_{kn}) \delta(\varepsilon_{k+qm}) \tag{6}$$

shows that the soft modes at points K and M are induced by Fermi surface nesting, and the soft modes along the L → A and H → A directions are induced by Kohn anomalies. Using the Allen and Dynes modified McMillan equation suitable for strong coupling[4], critical temperatures of 62, 77 and 79 K were predicted at 90, 120 and 160 GPa using calculated λ of 1.30, 12.0 and 1.29, respectively.

2.4. A perspective

We offered a glimpse on the relevant properties that affect superconductivity in high-pressure solids. It is shown that superconductivity is likely to occur in low-dimensional structures close to structural and dynamic instabilities. It is shown that the simultaneous existence of flat and steep electronic bands close to the Fermi level together with soft vibrational modes help to promote electron–phonon coupling. The characteristic features have also been observed in a growing number of superconductors [34], including the cuprates [36]. It is hoped that the discovery of superconductivity in high-pressure solids and recent exciting breakthroughs in other systems under ambient conditions [37] will eventually unlock the secret of high-T_c materials.

References

[1] Ashcroft N W 2002 *Nature* **419** 569
[2] Dacorogna M M, Chang K J and Cohen M L 1985 *Phys. Rev.* B **32** 1853
[3] Chang K J, Dacorogna M M, Cohen M L, Mignot J M, Chouteau G and Martinez G 1985 *Phys. Rev. Lett.* **54** 2375
[4] Eremets M I, Shimizu K, Kobayashi T C and Amaya K 1998 *Science* **281** 1333
[5] Takemura K, Sato K, Fujihisa H and Onoda M 2003 *Nature* **423** 971
[6] Shimizu K, Ishikawa H, Takao D, Yagi T and Amaya K 2002 *Nature* **419** 597
[7] Struzhkin V V, Eremets M I, Gan W, Mao H K and Hemley R J 2002 *Science* **198** 1213
[8] Deemyad S and Schilling J S 2003 *Phys. Rev. Lett.* **91** 167001
[9] Shimizu K, Kimura T, Furomot S, Takeda K, Kotani K, Onuki Y and Amaya K 2001 *Nature* **412** 316
[10] Yabuuchi T, Matsuoka T, Nakamoto Y and Shimizu K 2006 *J. Phys. Soc. Japan* **75** 083703
[11] Hamlin J J, Tissen V G and Schilling J S 2006 *Phys. Rev.* B **73** 094522
[12] Matthias B T 1955 *Phys. Rev.* **97** 74
[13] Migdal A B 1958 *Sov. Phys.—JETP* **34** 996
[14] Eliashberg G M 1960 *Zh. Eksp. Teor. Fiz.* **38** 966
Eliashberg G M 1960 *Sov. Phys.—JETP* **11** 696 (Engl. Transl.)
[15] Bardeen J, Cooper L N and Schrieffer J R 1957 *Phys. Rev.* **108** 1175
[16] Allen P B and Dynes R C 1975 *J. Phys. C: Solid State Phys.* **8** L158
[17] Savrasov S Y and Savrasov D Y 1996 *Phys. Rev.* B **54** 16487
[18] Nelmes R J, MaMahon M I, Loveday J S and Rekhi S 2002 *Phys. Rev. Lett.* **88** 155503
[19] MaMahon M I, Nelmes R J and Rekhi S 2001 *Phys. Rev. Lett.* **87** 055501
[20] MaMahon M I, Rekhi S and Nelmes R J 2001 *Phys. Rev. Lett.* **87** 255501
[21] Tse J S 2005 *Z. Kristallogr.* **220** 521
Katzke H and Toledano P 2005 *Phys. Rev.* B **71** 184101
[22] Hanfland M, Schwarz U, Syassen K and Takemura K 1999 *Phys. Rev. Lett.* **82** 1197
[23] Olijnyk H, Sikka S K and Holzapfel W B 1984 *Phys. Lett.* A **103** 137
[24] Duclos S J, Vohra Y K and Ruoff A L 1987 *Phys. Rev. Lett.* **58** 775
[25] Grünbaum B and Shephard G C 1986 *Tilings and Patterns* (New York: Freeman)
[26] Schwarz U, Takemura K, Hanfland M and Syassen K 1998 *Phys. Rev. Lett.* **81** 2711
[27] Takemura K, Shimomura O and Fujihisa H 1991 *Phys. Rev. Lett.* **66** 2014
[28] Tse J S, Klug D D, Patchkovskii S, Ma Y and Dewhurst J K 2006 *J. Phys. Chem.* B **110** 3721
[29] Tse J S, Ma Y and Tutuncu H M 2005 *J. Phys.: Condens. Matter* **17** S911

[4] We have used equation (8) in [16] which is applicable for strong coupling with $\lambda \leqslant 1.5$ to compute the critical temperature.

[30] Profeta G, Franchini C, Lathiotakis N N, Floris A, Sanna A, Marques M A L, Lüders M, Massidda S, Gross E K U and Continenza A 2006 *Phys. Rev. Lett.* **96** 047003
[31] Kasinathan D, Kune J, Lazicki A, Rosner H, Yoo C S, Scalettar R T and Pickett W E 2006 *Phys. Rev. Lett.* **96** 047004
[32] Rodriguez-Prieto A, Bergara A, Silkin V M and Echenique P M 2006 *Phys. Rev.* B **74** 172104
Xie Y, Tse J S, Cui T, Oganov A R, He Z, Ma Y and Zou G 2007 *Phys. Rev.* B **75** 064102
[33] Tse J S, Yao Y and Tanaka K 2007 *Phys. Rev. Lett.* **98** 117004
[34] For a review, see Deng S, Simon A and Kohler J 2005 *Struct. Bond.* **114** 103
[35] Wierzbowska M, de Grioncoli S and Giannozzi P 2005 *Preprint* cond-mat/0504077
[36] Dessau D S, Shen Z X, King D M, Marshall D S, Lombardo L W, Dickinson W P H, Loeser A G, DiCarlo J, Park C H, Kapitulnik A and Spicer W E 1993 *Phys. Rev. Lett.* **71** 2781
[37] Pickett W E 2006 *Preprint* cond-mat/0603428